



University of HUDDERSFIELD

University of Huddersfield Repository

Lane, Mark, Shaeboub, Abdulkarim, Gu, Fengshou and Ball, Andrew

Investigation of Reductions in Motor Efficiency caused by Stator Faults when operated from an Inverter Drive

Original Citation

Lane, Mark, Shaeboub, Abdulkarim, Gu, Fengshou and Ball, Andrew (2016) Investigation of Reductions in Motor Efficiency caused by Stator Faults when operated from an Inverter Drive. In: Proceedings 22nd International Conference on Automation and Computing (ICAC). IEEE. ISBN 9781862181328

This version is available at <http://eprints.hud.ac.uk/id/eprint/29509/>

The University Repository is a digital collection of the research output of the University, available on Open Access. Copyright and Moral Rights for the items on this site are retained by the individual author and/or other copyright owners. Users may access full items free of charge; copies of full text items generally can be reproduced, displayed or performed and given to third parties in any format or medium for personal research or study, educational or not-for-profit purposes without prior permission or charge, provided:

- The authors, title and full bibliographic details is credited in any copy;
- A hyperlink and/or URL is included for the original metadata page; and
- The content is not changed in any way.

For more information, including our policy and submission procedure, please contact the Repository Team at: E.mailbox@hud.ac.uk.

<http://eprints.hud.ac.uk/>

Investigation of Reductions in Motor Efficiency caused by Stator Faults when operated from an Inverter Drive

M. Lane A. Shaeboub F. Gu A.D. Ball
Centre for Efficiency and Performance Engineering
University of Huddersfield
Huddersfield, UK
mark.lane@hud.ac.uk

Abstract— Inverter driven motor systems have seen wider use in industry as energy reduction methods. Studies have been undertaken previously to understand the effects of voltage imbalances on motor efficiency and deratings. However, this has not been covered in much detail on inverter-driven motor systems. This paper aims to study the effect that motor stator resistance imbalances have on motor efficiency when used on inverter-driven systems. Motor imbalances may remain undetected by the inverter drive and can result in overheating and premature failure of the motor. Motor efficiency monitoring is now of greater interest due to new IEC standards defining new AC motor efficiency classes and this is also reviewed along with the standards for motor efficiency and inverter-operated motors.

Keywords— Asymmetry, Efficiency, Unbalanced, Stator resistance increase, Motor Current Signature Analysis (MCSA), Inverter Field Operated Controller (IFOC), Random switching pattern.

I. INTRODUCTION

The trend for installing inverter drives to increase efficiency of induction driven applications is widespread. However once the motor and drive is installed, there may be little or no attention paid to continued efficient operation of the system. Standard IEC 60034-30-1, published in March 2014 stipulates three efficiency levels for three-phase induction motors, IE1 to IE3. Phase 2 of the EU's efficiency level legislation (IE3) came into effect from 1 January 2015 stating that three-phase induction motors with a rated output from 7.5 to 375kW must now meet the IE3 efficiency level or IE2 when operated from an inverter drive. Furthermore, an updated standard IEC 60034-30-1 now includes for IE4 motors [1] operated directly on-line to the supply. Part 2 of this standard DD CLC/TS 60034-25:2008 [2] covers motors driven by inverter drives. The standard lists various factors that can affect motor efficiency when operated from inverter drives and these are listed in the standard. These are:

- Optimisation of motor flux depending on load
- Optimisation of pulse patterns
- Switching frequency

For fan/pump applications, the motor flux is reduced at low speeds because of the low torque requirements – this is usually termed ‘quadratic torque’ operation. The efficiency of an installation- can instantly be compromised if the engineer selects the wrong operating mode for the application. On the

motor test rig, the operating mode is constant torque because it is possible to apply full load to the motor across the operating speed range.

Figure 1 shows the relationship between inverter frequency and power losses in the motor, ΔP_L for different pulse frequencies f_p . Lower pulse frequencies lead to higher losses in the motor due to the effect of peak harmonic currents caused by the reduced switching cycle. Conversely, losses in the inverter increase with a higher switching frequency. It is therefore proposed to use the default switching frequency of 3KHz with the test inverter used for this study as a compromise between motor and inverter efficiency.

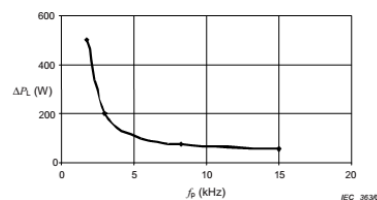


Fig. 1 Losses of motor due to switching frequency [2]

Factors that will affect motor life due to unequal stator resistances in operation are increased stress in the motor windings caused by the current and voltage imbalance which can then lead to increased motor losses and high running temperatures as a result of imbalanced current flows. This in turn can cause to torsional oscillation of the rotor, shortening the lifespan of equipment and consequentially in severe cases, mechanical failure [3]. The causes of stator resistance asymmetry are varied but can be linked to wiring connection corrosion due to atmospheric or mechanical effects in the drive or motor terminations, cable faults or poor installation techniques at the outset. Figure 2 gives the derating curve to apply when a percentage voltage unbalance is present.

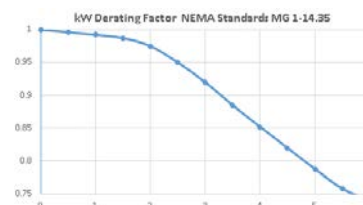


Fig. 2 NEMA Derating Curve to apply for voltage imbalances

If the reduction in motor efficiency can be measured and baselined at an early stage, it will be possible to maintain the equipment at the efficiency level it was when first installed.

There are advantages to industry if deteriorations in motor efficiency can be calculated by the inverter drive whilst the equipment is in-service.

G. A. McCoy [4] have published guidance notes for industry on maintaining efficiency of plant especially with regard to voltage unbalances. It is stated that voltage unbalances of even 1% require a motor to be derated. Resistance imbalances have the same effect and if unchecked can lead to premature motor failure. If consideration is also given to the heating effects that voltage imbalance can cause, it can be accepted that Montsinger's rule would apply which states that an increase in motor temperature by 10°C will lead to a reduction in the motor expected operational lifespan by 50%.

Studies by Jianghan Zhang [5] et. al. concerned the detection of open circuit faults in PWM converters using the motor current signals measured. This causes imbalance on the supply to the motor and the results of this are observed after transforming the a, b, c phase currents into the d, q reference frame for analysis. The diagnostic method was proved to work for single and double transistor open-circuit faults. However, a study into the motor efficiency reduction was not noted.

Sang Bin Lee [6] et. al. proposed a new strategy for condition monitoring of adjustable speed induction machine drive systems that could be used for off-line analysis of components such as DC link capacitors, electrical cabling, stator and cable insulation, stator core and rotor bar. The off-line technique does not require spectral analysis of the motor signals or have recourse to a motor mathematical model and by being an off-line test is independent of motor operating conditions such as frequency or load that have to be considered in an on-line system. Resistive imbalances can be measured when the motor is at standstill from the DC link voltage and this can help to benchmark motor connection conditions at stages in the motor operating life.

Camila P. Salomon et. al.[7] present work on induction motor efficiency evaluation using an air-gap torque method based on the sensorless torque equations developed and used particle swarm optimization methods on the data. This work was carried out on an inverter drive that was fed from a direct supply source. The output torque estimated using the calculations was compared to the mechanical output torque and considered a good approximation.

Yunhua Li et. al. [8] present a novel method to determine the motor efficiency under variable speed and partial load conditions. The model was tested on a healthy motor connected to an inverter drive with calculations based on the motor speed and power taken from the inverter drive standard analogue or digital communication outputs. The calculation errors for this model were found to be +/- 5% for 4-pole motors under constant speed conditions but the model accuracy is more uncertain at lower speed ratio conditions.

Motor Current Signature Analysis, MCSA is proven to reliably detect motor faults including winding inter-turn faults, air-gap eccentricity and broken rotor bars. Sharifi, R. et. al [9] combined MCSA and examination of Rotor Slot Harmonics to

diagnose inter-turn short-circuit faults in motor stator windings on non-inverter driven motors.

Rohan Samsi et. al. [10] studied the early detection of voltage imbalances in three-phase motors using pattern classification techniques such as Parks Vector Modulus with Wavelet analysis followed by pattern classification.

Further research by A Alwodai et. al. using MCSA [11] has also been considered with regard to detecting broken rotor bars and identify the distinctive features of frequency spectra associated with these faults.

This paper establishes that the efficiency and unbalance of an inverter-driven motor can be measured using the motor current and voltage signals measured using sensors connected between the drive and motor. Varying degrees of unbalanced conditions are measured against baseline motor data using post-signal processing techniques developed in MATLAB. Further signal processing techniques using spectral analysis are also applied to the data recorded and compared to other methods..

II. TEST FACILITIES AND FAULT SIMULATION

A. Test Rig

The test rig shown in Figure 3 is designed to have a test driving AC motor and a loading DC motor. The AC motor is a three-phase induction motor with rated output power P_r of 4 kW at a base speed N_{rated} of 1420 RPM (two-pole pairs). Motor rated current I_{rated} is 9.2A with magnetising current I_m of 5.2A. The AC motor is driven by a Parker 690 PWM inverter with 3 kHz switching frequency and a carrier frequency selected by a random pattern generator enabled by default. The drive is set to operate in sensorless vector control for all tests.

The DC motor is a shunt-wound design to apply different loading to the AC motor drive system. The speed, load and test duration are all programmable from a Siemens PLC thereby allowing for accurate and repeatable motor loading. The DC motor regenerates to the mains supply through a four-quadrant two phase DC drive.

Data is captured using a Sinocera 24Bit A/D Data Acquisition unit and imported into MATLAB for further processing.

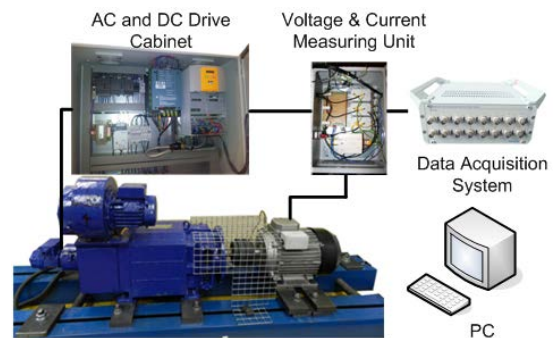


Fig. 3 Laboratory Test Rig

B. Operating conditions

The test cycle consists of five loading increments applied to a test motor running at a constant speed. Each of the five loading increments are repeated three times, making a total of 15 load steps as illustrated in Figure 4. An example plot is shown below this test step diagram to indicate how the test results are presented. Where vertical lines are shown in any plot, these represent the start of each new load test cycle.

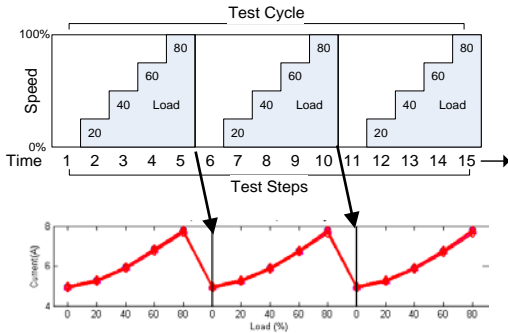


Fig. 4 Test cycle and example plot

The test run data detailing test run speeds, duration of test and AC motor loading is presented in Table I.

TABLE I. TEST CYCLE DATA

Step number	Speed RPM	Step duration(s)	Load (% of motor FLC)
1	1470	120	0
2	1470	120	20
3	1470	120	40
4	1470	120	60
5	1470	120	80

C. Motor baseline data

In order to construct a data set that can be used as a reliable comparison between a healthy motor and one with simulated faults, two separate test runs for the healthy motor were run with the motor up to full operating temperature (Mode 1 in Table II). The results of these test runs will be compared to check the robustness of the testing methods.

D. Fault Simulation

For comparative healthy and faulty motor data, the drive would be run for each test cycle in the following three modes as follows:

TABLE II. Drive operating modes

Drive Modes
1. Healthy motor auto-tuned
2. Motor with simulated stator fault of 0.2Ω
3. Motor with simulated stator fault of 0.4Ω

There are a number of phase resistance increments available on the test rig in 0.1Ω steps obtained by changing the wiring tapping on the custom-built resistor unit.

The resistance fault simulated is that which occurs in one winding inside the AC motor thereby affecting only one motor phase in a star-connected motor. This is indicated in Figure 5.

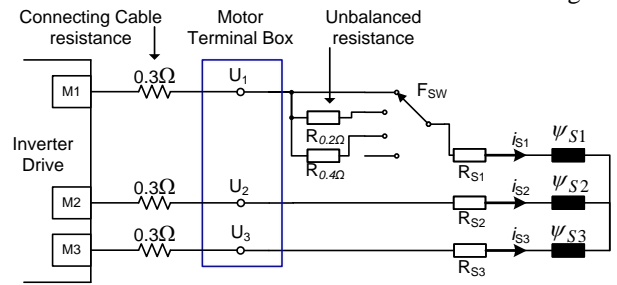


Fig. 5 Motor magnetising circuit detailing the stator phase resistance fault inserted in one of the three phase connections internally in the motor on phase 1 (STAR circuit)

The connecting cable resistance from drive to motor was measured at 0.3Ω for each phase. Therefore, at the maximum fault resistance introduced of 0.4Ω the total resistance between the drive and motor is increased from 0.3Ω to 0.7Ω in the faulty phase leg. The additional fault resistance inserted will be referred to as the resistance R_{fs} . The effect of a resistance increase in one phase of the stator equivalent circuit equation in a star connected machine is given by:

$$V_{s1} = R_s i_{s1} + \frac{d\psi_{s1}}{dt} \rightarrow V_{s1} = (R_{fs} + R_s) i_{s1} + \frac{d\psi_{s1}}{dt} \quad (1)$$

This imbalance created in the stator circuit has the effect of reducing the magnetic flux generated by one of the stator windings in proportion to the value of R_{fs} . The effect of this is to be studied for motor inefficiencies compared to normal running conditions.

It is proposed to use algorithms developed in MATLAB to calculate motor efficiency based on the following measurements taken from the test rig:

- Phase voltages a, b, c
- Phase currents a, b, c
- Motor speed

Motor temperature is also monitored and recorded so that the general operating conditions of the motor can be observed and ensure that the effect of motor temperature on the measured results is kept to an absolute minimum.

E. Effect on VSD Operation

To observe how the motor model in the sensorless PWM drive can be affected by a modification to stator resistance, the operation of an inverter model has been studied. The inverter drive in this test rig calculates the following values to use in the motor model during the autotune process:

Magnetizing inductance, L_M , Leakage Inductance $L_{\sigma s}$, Rotor Resistance R_R , Stator resistance R_S .

During drive operation, the test rig drive does not have an adaptive model to compensate for changes in stator resistance during operation. The model is only calculated once by the autotune function. To understand the influence of the motor

model on drive operation, a block diagram of a generic IFOC (Inverter Field Oriented Controller) inverter drive is given in Figure 6 [12].

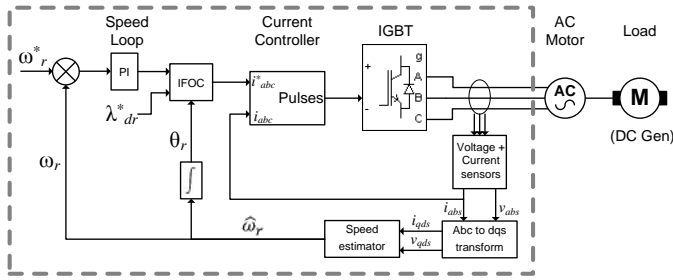


Fig. 6 Inverter FOC diagram

ω_r^* is the demanded speed, λ_{dr}^* the demanded rotor flux.

When calculating the current demand output from the IFOC current controller, feedback from the actual motor current and voltage signals are used after transformation from abc frame to dqs and from there to estimate the rotor angle θ_r . The frequency and voltage output from the inverter are therefore dependent on the rotor speed, predicted by the speed estimator. However, in order for the speed estimator to calculate speed accurately, the motor parameters stored in the drive for the motor model must correspond to the actual motor values.

For sensorless operation, estimated rotor speed $\hat{\omega}_r$ is calculated from the stator current and voltages based on the steady state equivalent circuit of an induction motor shown in Figure 7 is as follows:

$$\hat{\omega}_r = \frac{E}{\lambda_{dr}^{rf}} - \frac{R_r}{L_r} \cdot \frac{L_m \cdot i_{qs}^{rf}}{\lambda_{dr}^{rf}} \quad (2)$$

Where E , the air gap voltage is calculated based on the rotor stator resistance and inductance:

$$E = V_{qds} - R_s \cdot i_{qds} - \frac{d}{dt} \cdot L_{ls} \cdot i_{qds} \quad (3)$$

If the air gap voltage value is incorrect because the stator resistance R_s stored by the motor model in the drive is in error, then the rotor speed θ estimated by the drive will also be in error.

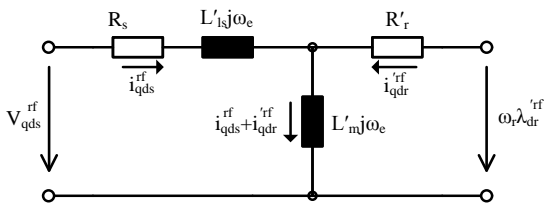


Fig.7 Induction motor steady state equivalent circuit

The simulated fault resistance should therefore not be compensated for by the drive controller and it is expected that motor performance will be affected by the faults introduced.

III. STATOR IMBALANCE SIMULATION TEST RESULTS

This section details and compares the test results obtained from the baseline tests and compares these to the simulated fault tests for stator resistance imbalances. It should be noted that the motor was brought up to normal operating temperature prior to the test results being commenced in line with recommendations from EN 60034-2-1:2014. [13].

A. Motor Terminal Voltage and Phase Current

Following a period of prolonged running at 80% load a stable motor operating temperature was reached. The worst case temperature difference was recorded at 5°C across all tests.

A plot of motor voltage, current and speed was taken at each load increment but minimal difference between healthy and fault conditions was observed until the motor reached 80% loading. Figure 8 presents a plot of motor voltage, current and speed measured at the 80% load point with 100% speed applied. From this, it can be observed that the voltage and current readings for each phase are more dispersed under unbalanced conditions.

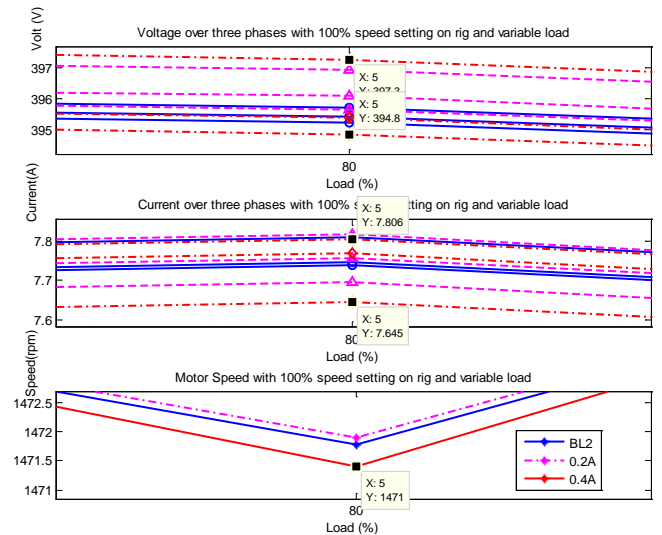


Fig. 8 Plot of voltage, current and speed over 3 phases at 80% load condition with 100% speed setting. BL2 = Baseline (Healthy Motor); 0.2A = Stator Resistance imbalance of 0.2Ω; 0.4A = Stator Resistance imbalance of 0.4Ω.

B. Motor Current and Voltage Asymmetry

Figure 9 indicates the results of calculating motor voltage and current imbalances across all phases in accordance with the NEMA definition. This defines the Line Voltage Unbalance Rate (LVUR) as:

$$LVUR = \frac{\text{maximum deviation from line voltage}}{\text{average line voltage}} \quad (4)$$

$$LVUR = \frac{\max[(U_{ab} - U_{lavg}), (U_{bc} - U_{lavg}), (U_{ca} - U_{lavg})]}{U_{lavg}} \quad (5)$$

Where U_{ab} , U_{bc} and U_{ca} are line voltages.

The same method is applied to measure the difference in motor currents using the NEMA definition. The current and voltage readings show that there is a noticeable difference in current and voltage imbalances when the fault resistance is introduced. The maximum is 1.068V at 80% loading for the 0.4Ω fault resistance.

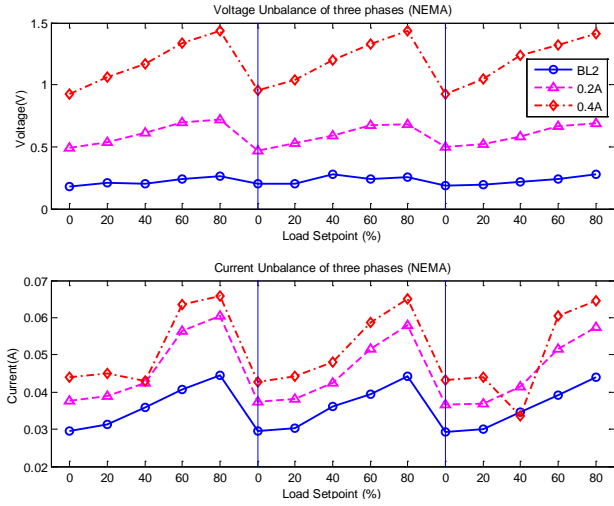


Fig. 9 Voltage and current imbalances under NEMA definitions

C. Motor Efficiency

Figure 10 plots the results of the motor efficiency calculations based on shaft power estimation, electrical input power estimation and power based on the no load current method. Instantaneous input power of an ac motor is calculated as: $P = V_a I_{sa} + V_b I_{sb} + V_c I_{sc}$ (6)

An average value of the instantaneous power is taken for these efficiency calculations. The shaft power is calculated as:

$$P_s = \left[\frac{1}{3} \left(\frac{\sigma(\overline{I_{sa}}) + \sigma(\overline{I_{sb}}) + \sigma(\overline{I_{sc}})}{I_{rated} \cdot P_{rated} \cdot \frac{\omega_m}{\omega_{rated}}} \right) \right] \quad (7)$$

Where i_{a_avg} represents the averaged current samples for i_a . ω represents speed in revolutions per second.

The electrical input power calculation is based on the mean value of all the measured current signal samples calculated by

$$P_i = \overline{(V_a I_{sa} + V_b I_{sb} + V_c I_{sc})} \quad (8)$$

Efficiency by current method uses the standard deviation of all data points for i_a, i_b, i_c with filter windows applied to calculate a single current value I_{abc} at each data sample point.

$$I_{abc} = \frac{1}{3} \sigma(\overline{I_{sa}}) + \sigma(\overline{I_{sb}}) + \sigma(\overline{I_{sc}}) \quad (9)$$

Based on the nameplate motor power rating, P_r a theoretical power output P_o is calculated based on the actual measured motor speed.

From these results, the efficiency η_l is calculated as

$$\eta_l = \left[\left(\frac{2 \cdot (I_{abc} - I_m)}{2 \cdot I_{sr} - I_m} \right) \cdot \frac{P_r}{P_i} \right] \quad (10)$$

Where I_m is the magnetising current, I_{sr} is the stator rated current. The results are inconclusive at motor loads below 60% but from this point to 80% load, there is a consistency to the results where the baseline data shows increased output power, input power and efficiency compared to the unbalanced results. Efficiency is reduced by approximately 0.2% from the faulty motor compared to baseline.

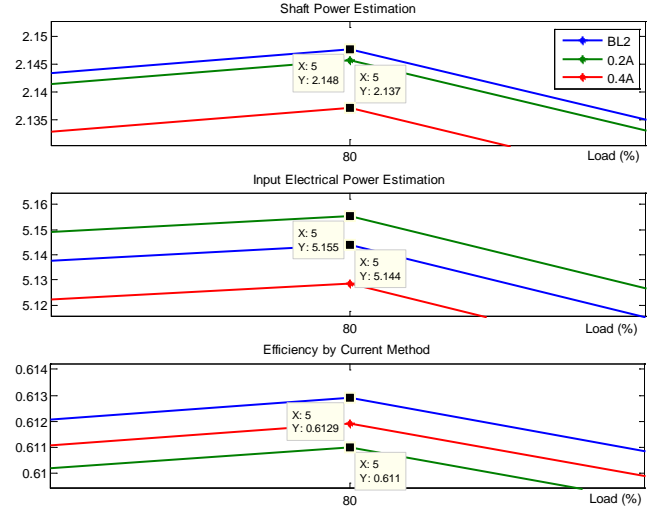


Fig. 10 Motor efficiency calculations at 80% loading

D. Motor Efficiency by Air Gap Torque Method

Figure 11 presents the efficiency, η calculations based on the air gap torque method. The air gap torque T_{ag} is calculated after subtracting the stator resistance, core and stator stray losses. The following voltage equations apply for all stator windings where R_s is the stator (phase) resistance

$$v_{a,b,c} = \frac{d\psi_{a,b,c}}{dt} + R_s \cdot i_{a,b,c} \quad (11)$$

The air gap torque T_{ag} calculation used is given below [14]:

$$T_{ag} (Nm) = \frac{P}{2 \cdot \sqrt{3}} \left\{ \begin{aligned} & (i_A - i_B) \cdot \int [v_{CA} - R(i_C - i_A)] dt \\ & - (i_C - i_A) \cdot \int [v_{AB} - R(i_A - i_B)] dt \end{aligned} \right\} \quad (12)$$

The efficiency calculation is expressed as

$$\eta = \frac{T_{sh} \cdot \omega_r}{P_{in}} = \frac{T_{ag} \cdot \omega_r - W_{fw} - W_{LLr}}{P_{input}} \quad (13).$$

Where W_{fw} is the friction and windage loss and W_{LLr} the rotor stray losses.

At full load, the air gap torque efficiency calculations indicate an increased efficiency in the motor with unbalanced

stator windings until the motor is loaded up to 80%. However, the efficiency calculations do not take into account the additional fault resistance introduced.

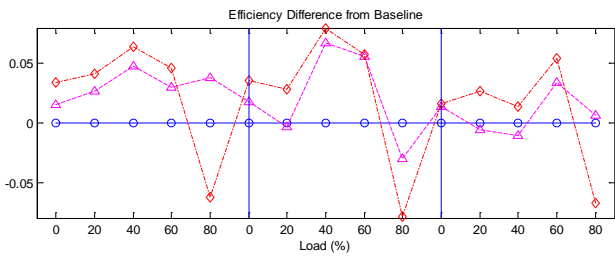


Fig. 11 Motor efficiency calculations using air gap torque method

When the baseline data is taken as the reference point for efficiency measurements, the difference can be observed in more detail.

E. Motor Current Spectral Analysis

Figure 12 presents a comparison of current spectrum between the different operating modes at the maximum motor speed of 1470 RPM. It shows that the 3rd harmonic is increased for the two faulty modes at full speed and at 80% load.

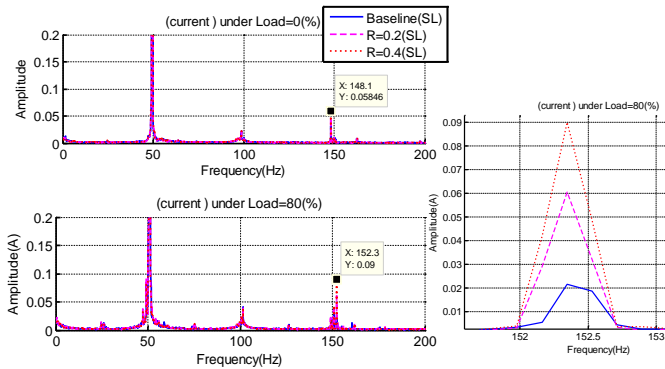


Fig. 12 Frequency spectral plot of motor current signals under 0% and 80% load.

IV. CONCLUSIONS

This paper has demonstrated that it is possible to use motor current and voltage signals output from a PWM converter to differentiate between a healthy motor and a motor developing a graduated imbalanced fault on one stator winding.

The results show that the NEMA method of calculating imbalanced current and voltages is most effective under imbalanced fault conditions and for a wide range of loads. An advantage of the NEMA method is that the reference data set could be sampled with the motor in service and under a range of load conditions. This method consistently indicated an increase in imbalance for current and voltage for all load ranges at a constant speed. Efficiency reductions of 0.2% as observed in figure 8 would not be cause for concern under general operation and may be difficult to detect in real-world conditions. If it is proven that the techniques are sensitive enough to detect this reduction in efficiency reliably and repeatedly then field tests can be carried out to signal faults at efficiency losses greater than 5%. From Figure 2 this equates to a voltage unbalance of 2.5%. In experimental tests carried out

for this paper, the maximum voltage unbalance measured was 10 times less at 0.267%.

It has been shown that the motor current spectral signal analysis method has been shown to be a reliable indicator when the motor is running at close to rated loads and is an alternative to the time-domain analysis for detecting the severity of the fault.

The efficiency calculations are less conclusive for reduced motor loads but it is well known that motors are less efficient when operating under reduced load conditions and in general, motors should be sized to operate towards their full load rating to maximise efficiency of the installation. Therefore, the efficiency calculation method could be chosen for applications that run the motor towards the full-load area for greater effectiveness.

REFERENCES

- [1] Efficiency classes for IEC line motors. www.siemens.com/international-efficiency
- [2] DD CLC/TS 60034-25:2008 Rotating electrical machines. Guidance for the design and performance of a.c. motors specifically designed for converter supply
- [3] Mirabbasi, D., G. Seifossadat, and M. Heidari. Effect of unbalanced voltage on operation of induction motors and its detection. IEEE International Conference on Electrical and Electronics Engineering, 2009.
- [4] Gilbert A. McCoy and John G. Douglass, Washington State University; Energy Management for Motor-Driven Systems Revision 2 March 2000
- [5] Jiangnan Zhang, Jin Zhao, Dehong Zhou, and Chengguang Huang, High-Performance Fault Diagnosis in PWM Voltage-Source Inverters for Vector-Controlled Induction Motor Drives, IEEE Transactions On Power Electronics, Vol. 29, No. 11, November 2014
- [6] Sang Bin Lee, Jinkyu Yang, Jongman Hong, et al. A New Strategy for Condition Monitoring of Adjustable Speed Induction Machine Drive Systems, IEEE Transactions On Power Electronics, Vol. 26, No. 2, February 2011
- [7] Camila P. Salomon, Wilson C. Sant'Ana, Luiz E. Borges da Silva, Germano Lambert-Torres et. al. Induction Motor Efficiency Evaluation Using a New Concept of Stator Resistance IEEE Transactions On Instrumentation And Measurement, Vol. 64, No. 11, November 2015
- [8] Yunhua Li, Mingsheng Liu, Josephine Lau, Bei Zhang, A novel method to determine the motor efficiency under variable speed operations and partial load conditions, Bes-Tech Inc., Omaha, NE 68117, USA,
- [9] Sharifi, R. and M. Ebrahimi, Detection of stator winding faults in induction motors using three-phase current monitoring. ISA transactions, 2011. 50(1): p. 14-20.
- [10] Rohan Samsi, Venkatesh Rajagopalan, Jeffrey Mayer, Asok Ray, et. al. (2005) Early Detection of Voltage Imbalances in Three-Phase Induction Motors; 2005 American Control Conference June 8-10, 2005. Portland, OR, USA
- [11] Alwodai, A, Gu, Fengshou and Ball, Andrew; A Comparison of Different Techniques for Induction Motor Rotor Fault Diagnosis. Mechanical Systems and Signal Processing 50-51 (2015) p. 400-413
- [12] Mohamed S. Zaky (2012) Stability Analysis of Speed and Stator Resistance Estimators for Sensorless Induction Motor Drives. IEEE Transactions On Industrial Electronics, Vol. 59, No. 2, February 2012
- [13] BS EN 60034-2-1:2014 Rotating electrical machines Part 2-1: Standard methods for determining losses and efficiency from tests (excluding machines for traction vehicles)
- [14] Bin Lu, Thomas G. Habetler, Ronald G. Harley (2008) A Nonintrusive and In-Service Motor-Efficiency Estimation Method Using Air-Gap Torque With Considerations of Condition Monitoring. IEEE Transactions On Industry Applications, Vol. 44, No. 6, November/December 2008